Alvaredo, P., Roa, J. J., Jiménez-Pique, E., Llanes, L., & Gordo, E. (2017). Characterization of interfaces between TiCN and iron-base binders. International Journal of Refractory Metals and Hard Materials, 63, 32-37.

doi:https://doi.org/10.1016/j.ijrmhm.2016.08.010

Characterization of interfaces between TiCN and iron-base binders

P. Alvaredo[1], J.J. Roa[2, 3], E. Jiménez-Pique[2, 3], L. Llanes[2, 3], E. Gordo[1]

[1]Department of Materials Science and Engineering, IMAAB. University Carlos III of Madrid, Avda. Universidad, 30, 28911 Leganés, Madrid, Spain
[2]Department of Materials Science and Engineering, CIEFMA. Polytechnic University of Catalonia, Avda. Diagonal 647, 08028 Barcelona, Spain.
[3]CRnE, Campus Diagonal Sud, Edificio C', Polytechnic University of Catalonia, C/ Pascual i Vila 15, 08028 Barcelona, Spain.

Abstract

This work includes a study of the interface between matrix and reinforcement in Fe-Ti(C,N) systems. A study of wettability and solubility between metal and ceramic phases is first performed. It combines wetting experiments at high temperature with kinetics simulation. In doing so, dense Ti(C,N) is produced by spark plasma sintering and used as substrate. On the other hand, Fe, Fe-WC and Fe-Mo_2C alloys are used as metal matrix to evaluate the influence of WC and Mo_2C carbides on the formation, composition and properties of the interface. These experiments are complemented by a micromechanical study of the interface. Hardness and elastic modulus are obtained from analysis of nanoindentation arrays in the matrix and into the reinforcement for each system. The sliding contact response at the interface (and neighboring regions) is evaluated by cross-section nanoscratches conducted at different load levels.

1. Introduction

Several studies have been conducted on a TiCN-based cermet with a high speed steel as metallic matrix. Results obtained show high values of hardness and toughness [1], as well as good oxidation response at high temperature and wear resistance [2, 3]. Main reasons for choosing a Fe alloy to replace the conventional Ni and Co used as metallic matrix in this type of composites are its lower price and toxicity, in addition to the possibility to adapt its properties to intended applications by means of heat treatment. A commercial high speed steel has been chosen because it contains alloying elements such as W and Mo, known to be carbides formers. Furthermore, the presence of carbides of transition elements in cermets not only increases the proportion of hard phase of the composite material but also improves the sinterability of them because they play a key role in the solubility between matrix and reinforcement.

The processing of TiCN-based cermets is performed by Liquid Phase Sintering (LPS) and leads to the typical *core-rim* microstructure of Ti(C,N)-based cermets. This microstructure is formed during the sintering, where solid ceramic grains coexist with the liquid metal. As a result, Ti(C,N) particles are first wetted and partially dissolved by the liquid, but later precipitate again enriched in transition elements from the secondary refractory carbides. The terms *core* and *rim* correspond with undissolved Ti(C,N) and solid solution (Ti,M)(C,N) respectively, being *M* the transition metal from the refractory carbides as WC and Mo_2C. The presence of this *rim* strongly affects the mechanical properties of the cermet. Its formation, composition and thickness depend on the solubility of the reinforcement particles on the liquid metal and the mechanisms taking place during sintering [4-6].

The solubility processes during sintering strongly affect the formation of the interface between metallic and ceramic phases. They are also critical for developing the final microstructure and properties of the cermet. Within this context, this work presents an investigation of the interface of cermet systems where Fe-base matrices coexist with Ti(C,N) reinforcements. A study of wettability and solubility between metal and ceramic phases is first performed. It combines wetting experiments at high temperature with kinetics simulation. In doing so, dense Ti(C,N) was produced by spark plasma sintering (SPS) and used as substrate. On the other hand, Fe, Fe-WC and Fe-Mo_2C alloys were used as metal matrix to evaluate the influence of WC and Mo_2C carbides added to the Fe matrix on the formation, composition and micromechanical properties of the interface. Hardness and elastic modulus have been obtained by using the

nanoindentation technique in a region near the interface for each system. Finally, the sliding contact response close to and at the interface has been evaluated by cross-section nanoscratches, from the matrix into the reinforcement, carried out at different load levels.

2. Materials and methodology

The powders used as starting materials in this work are: $TiC_{0.5}N_{0.5}$ (H. C. Starck), Fe (Ecka granules), WC (Alfa Aesar), Mo (Aldrich) and graphite. To study the influence of WC and Mo_2C, the compositions studied correspond with carbide amounts in high speed steel M2 used in previous works [1,3]. Therefore the compositions of the metallic samples studied are Fe, Fe-6.6WC and Fe-5.1Mo_2C.

The simulation of high temperature solubility at the interface between the liquid metal sample (Fe, Fe-6.6WC and Fe-5.1Mo_2C) and TiCN solid substrate is performed by using the software Dictra with the TCFE7 database. The design of the system used in the simulation is shown in Figure 1. There are two regions: a left one corresponding with the liquid metal sample and a right one corresponding with the TiCN solid substrate. The simulated distance is around 100 μm and the simulation times are: 1, 10, 100 and 1000 s. The temperature at which simulation has been performed is 1560 ºC, in order to have the metallic sample in liquid state. In the case of Fe sample, it is always in liquid state at 1560 ºC, because the melting point of Fe is 1538 ºC. In the others systems, the binary phase diagram of Fe-6.6WC and Fe-5.1Mo_2C calculated by Thermocalc software [7] (Figure 2), confirms that these two compositions are in liquid state at the simulation temperature. Calculations are based on the free Gibbs energy minimization code and mass conversion rule in combination with TCFE7 database (Scientific Group Thermodata Europe).

Figure 1. Scheme of the system designed for the simulation of the diffusion (at the interface) between the liquid metallic sample and the solid ceramic substrate.
Figure 2. Binary phase diagrams of Fe-WC (left) and Fe-Mo_2C (right), calculated by Thermocalc software.

Aiming to assess the wettability of metal samples on ceramic substrates, wetting experiments at high temperature have been performed. They were conducted in a tubular furnace under Ar atmosphere. A camera is externally adapted to the furnace, to record the evolution of the shape of the drop of liquid metal on the substrate. The scheme of the equipment is shown in Figure 3. The evolution of the contact angle between the two phases as a function of the residence time and temperature is monitored by the sessile drop method.

Figure 3. Scheme of the high temperature contact angle measurement equipment.

The metal samples were previously sintered under vacuum atmosphere at 1450 ºC during 1 hour. The TiCN substrates were sintered by SPS at 1900 ºC and a pressure of 70 MPa with a heating and cooling rate of 100 ºC/min. Final relative density was 99.5 %.

After the wetting experiments, samples were mounted, transversally cut, ground and polished until mirror polish condition. The resulting cross section between metal sample and ceramic substrate was observed by Scanning Electron Microscope (SEM) and analyzed by energy dispersive X-ray spectroscopy (EDX).

Prior to micromechanical characterization, the specimens were re-polished with colloidal silica, in an ordinary metallographic polisher. The quality of the finishing was checked by confocal laser scanning microscopy (CLSM, LEXT OLS3100) in order to avoid the presence of scratches on the surface prior to testing. After that, the surface to be tested was cleaned using a non-ionic surfactant (detergent) and afterwards dried with pure air.

The micromechanical properties in a region near the interface for each system included the evaluation of their hardness (*H*) and elastic modulus (*E*) through Nanoindentation technique. It was performed using a nanoindenter XP (MTS) equipped with a continuous stiffness measurement (CSM) modulus, the latter allowing a dynamic determination of hardness and elastic modulus during the indentation [8]. Indentations were organized in a homogeneous spaced array of 16 indentations (4 by 4) at 1000 nm of maximum displacement into surface. Indentation array was located in a region near the interface with a constant distance between

each residual imprint of 50 μm in order to avoid any overlapping effect. Strain rate through was kept constant at 0.05 s^{-1} during the nanoindentation test. The indenter shape was carefully calibrated by indenting standard sample of known Young's modulus (Fused Silica, 72 GPa). The hardness and elastic modulus were determined by using the Oliver and Pharr method [9], assuming a constant Poisson ratio for the specimens equals to 0.3.

Sliding contact tests were done at micrometric length scale by using the nanoindenter system referred above. A Berkovich indenter was employed to scratch the interfaces from the TiCN substrate into the reinforcement. A Berkovich indenter was employed to scratch the interface at incremental (from 0 up to 100 mN) and constant applied load (100 mN), at a constant scratch velocity of 10 μm/s. Three different scans were done in each sample with a scratch length of 200 μm and in an interval between them of the same length of the scratch. More information about the sliding method is available in Ref. [10].

Surface damage associated with residual nanoindentation imprints and nanoscratchs were visualized by field emission scanning electron microscope (FESEM, JEOL-7100F) at 20 kV.

3. Results

Figure 4 shows the evolution of the contact angle of the systems Fe/TiCN, Fe-6.6WC/TiCN and Fe-5.1Mo_2C/TiCN as a function of the residence time. The results are shown such that t = 0 s corresponds to the instant where formation of the liquid phase of the metallic sample is first observed. It is seen that liquid Fe does not wet the TiCN substrate. It forms a 100° contact angle which does not change with time. On the other hand, Fe-6.6WC and 5.1Mo_2C exhibits a clearly improved wettability behavior on the TiCN substrate. Contact angle for these systems is always lower than 100º, yielding final values of 70º and 38º for Fe-6.6WC and 5.1Mo_2C, respectively.

Figure 4. Evolution of contact angle regarding time of the metal/substrate systems: Fe/TiCN; Fe-6.2WC/TiCN and Fe-5.1Mo_2C/TiCN.

The diffusion simulation, performed by means of Dictra, allows to understand their interaction at high temperature and to explain the differences found in the wetting behavior. Figure 5 shows the interfaces of the systems - Fe/TiCN; (Fe+6.6WC)/TiCN and (Fe+5.1Mo_2C)/TiCN - formed during the wetting experiments, and the EDX analysis of the metallic sample, interface and substrate. Moreover, the diffusion of C and N, and W and Mo, as simulated by Dictra, is shown in Figure 6 and Figure 7.

For the Fe/TiCN system, it is observed that the substrate is not dissolved by the Fe sample. This phenomenon may be attributed to a diffusion process of C into the Fe sample. Such a behavior is also evidenced in Figure 6 in which the percentage of N is increased and the percentage of C is decreased at the interface. For the system (Fe+6.2WC)/TiCN, a clear dissolution of the TiCN substrate is evidenced at the interface. EDX analysis through the interface reveals two features: *(i)* reduction of C wt. % content with respect to the substrate composition, and *(ii)* a diffusion mechanism due to the presence of W element. Both effects are also observed in the Dictra results presented in Figure 6 and 7, respectively. The analysis of the interface could indicate the formation of a (Ti, W)(C, N) solid solution, which is characteristic of the *rim* phase in cermets. The interface of the system (Fe+5.1Mo_2C)/TiCN also shows a relative high solubility of the TiCN substrate on the alloy sample. EDX analysis shows the reduction of the C wt. % content and the presence of Mo, which is observed in the results obtained by doing simulation and represented in Figure 7. This analysis highlights the formation of the (Ti, Mo)(C, N) solid solution.

Samples with WC and Mo_2C present a slightly better wettability on TiCN substrate, as compared to that exhibited by the Fe sample. This effect may be attributed to several factors: *(i)* an increase of the solubility of TiCN in the liquid alloy, and/or *(ii)* a change in surface energy which allows a reduction of the contact angle improving the spreading of the liquid phase on the TiCN substrate.

Figure 5. Interface of the systems (left side): Fe/TiCN; Fe-6.2WC/TiCN and Fe-4.8Mo_2C/TiCN after wetting experiments and EDX analysis of metallic sample, interface and TiCN substrate (right side). (All the compositions are expressed in wt. %).

Figure 6. Evolution of the C and N wt. % at the interface for the systems Fe/TiCN; Fe-6.6WC/TiCN and Fe-5.1Mo_2C/TiCN simulated by Dictra software (at 1560 °C in a distance of 100 µm during 300 s).
Figure 7. Evolution of the W and Mo wt. % at the interface of the systems Fe-6.6WC/TiCN and Fe-5.1Mo_2C/TiCN, respectively, simulated by Dictra software (at 1560 °C in a distance of 100 µm during 300 s).

The improvement on the wettability by the addition of W and Mo carbides would be reflected in an improvement on the sinterability of the cermet getting higher densification during LPS. Additionally, the increasing of the TiCN solubility and the formation of the (Ti, M)(C,N) solid solution would lead to a smaller grain growth and agglomeration of the reinforcement particles. Beside these mentioned changes, the presence of W and Mo carbides could be expected to affects the mechanical properties of the material and the adhesive strength of matrix and reinforcement at the interface.

The micromechanical properties, in terms of hardness as a function of the maximum displacement into surface, for each liquid metal sample as well as for the TiCN substrate are shown in **Figure 8**. Hardness is nearly constant for displacements into the surface inside the interval 100 – 1000 nm. For lower penetrations, changes in hardness are extremely complicated to estimate due to several factors: *(i)* the influence of the superficial defects (i.e. roughness, residual stresses, among others), and *(ii)* the bluntness of the Berkovich tip indenter. Therefore, unless otherwise stated, the indentation hardness presented in **Table 1** is referred to this displacement interval.

The elastic modulus values reported in **Table 1** have been determined at 200 nm, where this property is constant, due to negligible interaction of the elastic field with the interface. As it can be appreciated in this table, the elastic modulus for the liquid metal sample is around 205 GPa. On the other hand, the TiCN substrate is slightly stiffer, yielding a value of 350 GPa.

As it is shown in Table 1, hardness values for the reinforcement range between 2 and 9 GPa for the Fe and Fe-Mo_2C systems, respectively. Meanwhile, for the Fe-WC system, hardness values are closer to those obtained for the Fe system. This trend can be attributed to two different factors: differences on intrinsic hardness and/or on density for the reinforcement particles (WC and/or Mo_2C). As it was reported by Nino and co-workers, at low applied loads the Vickers' hardness for both systems is around 20 GPa [11]. Then, differences determined for the Fe-WC and the Fe-Mo_2C systems should be related to microstructural assemblage differences in terms of density. Then, this parameter will govern the amount of particles heterogeneously distributed as reinforcement. Considering that density of Mo_2C is about half that of WC (15.7 and 8.9 g/cm^3 for WC and Mo_2C respectively), relative amount of Mo_2C may be expected to be much higher than that of WC. Accordingly, measured hardness values are also higher for Fe-Mo2C system than for the Fe-WC one.

Table 1. Hardness (determined from the hardness average for the displacement interval ranged between 100 – 1000 nm) and elastic modulus (at 200 nm) for the TiCN substrate and each metal liquid sample.

Figure 8. Hardness evolution for all the systems of study against the maximum displacement into surface.

Figure 9 exhibits images obtained by FESEM for Fe and Fe-Mo_2C liquid metal specimens. As seen in these images, the Fe imprint present a pile-up effect surrounding the residual indentation (see white arrows) due to their ductile behavior. On the other hand, the imprint done in the Fe-Mo_2C system does not present this effect, pointing out that this metal system is harder than the Fe system. No microcracks generated during the indentation process can be appreciated either. These observations are in agreement with the data presented in **Figure 8** and summarized in **Table 1** for both systems.

Figure 9. FESEM image of a residual imprint performed at 1000 nm of maximum displacement into surface for Fe and Fe-Mo_2C metallic systems.

In the scratch test there is a large shear stress on the surface caused by friction between the material and the indenter. Figure 10 shows an entire scratch track for the Fe/TiCN system passing through the interface (left hand side) for an incremental load experiment (from 0 up to 100 mN of maximum sliding load). In the right hand side of this image, it is possible to appreciate a magnification from the top-view FESEM of nanoscratches tracks for each system

investigated here at constant load (~ 100 mN). As it can be depicted in this image, damage events, location of damage features changes from the metallic into the ceramic phase when comparing the Fe/TiCN system with the other two systems (Fe-6.2WC/TiCN and Fe-5.1Mo_2C/TiCN). However, in all the cases damage may be defined as cohesive (although close to the interface) and not adhesive, pointing out satisfactory levels of adhesion strength for the three systems studied. This is particularly true for the Fe-Mo_2C/TiCN where mechanical integrity at the interface is neatly observed. The transition on the location of the damage features, as referred above, is here captured because nanoscratch testing was conducted from the matrix into the reinforcement, and should be related to the gradual changes in chemical composition, and consequent hardness and brittleness increase, present in the vicinity of the interface for Fe-6.2WC/TiCN and Fe-5.1Mo_2C/TiCN systems. Similar damage scenario was observed for the sliding tests done at incremental load (0 to 100 mN); thus, they are not presented again. It means that fracture events induced under sliding conditions do not depend on the applied stress, but rather on the chemical and microstructural nature of regions neighboring the interface.

Figure 10. FESEM image for the nanoscratch track performed at incremental load from 0 to 100 mN (left hand side) for the Fe/TiCN system. Magnification of the main fracture events activated in the interface for all the systems investigated here done at constant load (100 mN).

4. Conclusions

Chemically and mechanical interface characterization of iron-matrix cermets was studied by considering three different systems: Fe/TiCN; Fe-WC/TiCN and Fe-Mo_2C/TiCN. The main conclusions resulting from the study can be summarized as follows:

i) Carbide additions results in an enhanced wetting behavior, possibly as a result of a simple change of the interface composition. It would either modify the surface energy between solid and liquid phases, decreasing the contact angle; or increase the substrate solubility on the metallic sample, leading then to a higher dissolution of the substrate and a better spreading of the liquid sample.

ii) The TiCN substrate is harder and stiffer than the alloys evaluated here. As Fe-base matrices include WC and Mo2C contents, an increase of both properties is attained, as compared to pure Fe reinforcement.

iii) Nanoscratch testing (using a sharp indenter tip) results in a change in the location of damage events, from the ceramic to the metallic phase, when comparing the Fe-TiCN systems with the Fe-WC/TiCN and Fe-Mo2C/TiCN ones. However, in all the cases damage discerned is rather cohesive and not adhesive, this being quite clear for the Fe-Mo2C/TiCN system. Such a response is related to the gradual chemical composition changes (and consequent hardness and brittleness increase) in regions close to the interface.

iv) Damage scenarios induced during the sliding tests are independent of the stress stare associated with sliding contact loads.

Acknowledgements

The authors would like to acknowledge the financial support from the Spanish Government through the project MAT2012-38650-C02-01 and MAT-2012-34602, the Regional Government of Madrid through the program MULTIMAT-CHALLENGE, ref. S2013/MIT-2862. Dr. J.J.Roa would like to thank the "*Juan de la Cierva*" Programme for its financial support (grant number: JCI-2012-14454).

References

[1] P. Alvaredo, D. Mari, E. Gordo, International Journal of Refractory Metals and Hard Materials, 41 (2013) 115-120.

[2] B. Gómez, A. Jiménez-Suarez, E. Gordo, International Journal of Refractory Metals and Hard Materials, 27 (2009) 360-366.

[3] P. Alvaredo, C. Abajo, S.A. Tsipas, E. Gordo, Journal of Alloys and Compounds, 591 (2014) 72-79.

[4] E. Chicardi, Y. Torres, M.J. Sayagués, V. Medri, C. Melandri, J.M. Córdoba, F.J. Gotor, Chemical Engineering Journal, 267 (2015) 297-305.

[5] H. Yu, Y. Liu, Y. Jin, J. Ye, International Journal of Refractory Metals and Hard Materials, 29 (2011) 586-590.

[6] J. Jung, S. Kang, Acta Materialia, 52 (2004) 1379-1386.

[7] J.O. Andersson, T. Helander, L. Höglund, P. Shi, B. Sundman, Calphad, 26 (2002) 273-312.

[8] W.C. Oliver, G.M. Pharr, Journal of Materials Research, 19 (2004) 3-20.

[9] W.C. Oliver, G.M. Pharr, Journal of Materials Research, 7 (1992) 1564-1583.

[10] C.A.Botero, E.Jiménez-Piqué, R.Martín, T.Kulkarni, V.K.Sarin, L.Llanes, Surface and Coatings Technology, 239 (2012) 49-57.

[11] A.Nino, A.Tanaka, S.Sugiyama, H.Taimatsu, Materials Transactions, 51 (2010) 1621.

Table 1. Hardness (determined from the hardness average for the displacement interval ranged between 100 – 1000 nm) and elastic modulus (at 200 nm) for the TiCN substrate and each metal liquid sample.

Sample	**Hardness, H (GPa)**	**Elastic modulus, E (GPa)**
TiCN	19.17 ± 1.19	354 ± 86
Fe	2.25 ± 0.18	204 ± 5
Fe-Mo_2C	9.27 ± 0.39	203 ± 34
Fe-WC	3.17 ± 0.19	212 ± 27

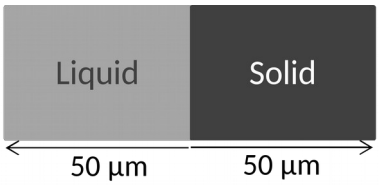

Figure 1. Scheme of the system designed for the simulation of the diffusion (at the interface) between the liquid metallic sample and the solid ceramic substrate.

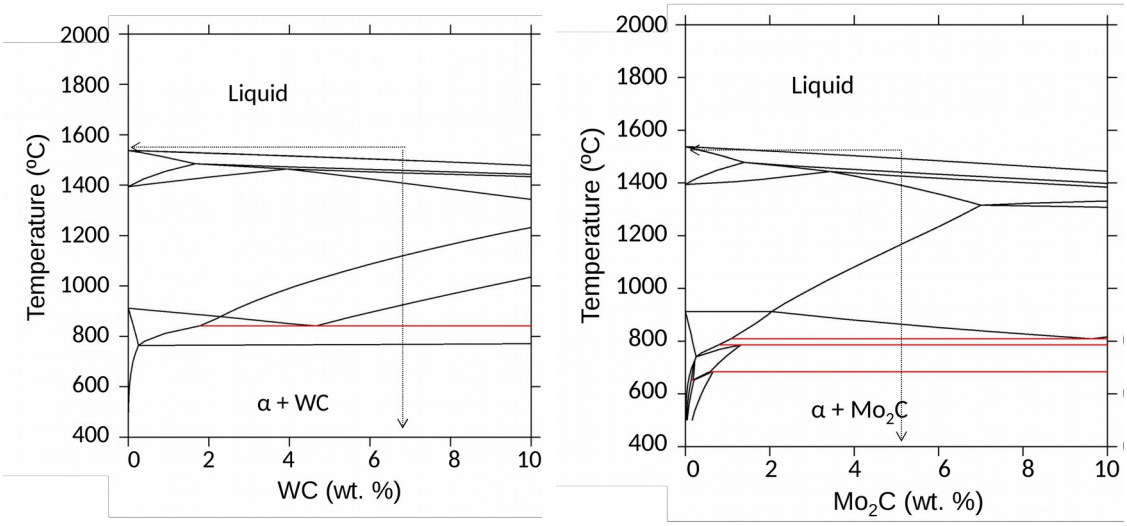

Figure 2. Binary phase diagrams of Fe-WC (left) and Fe-Mo_2C (right), calculated by Thermocalc software.

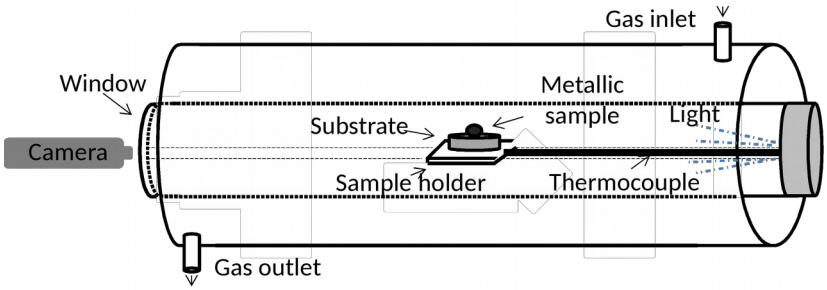

Figure 3. Scheme of the high temperature contact angle measurement equipment.

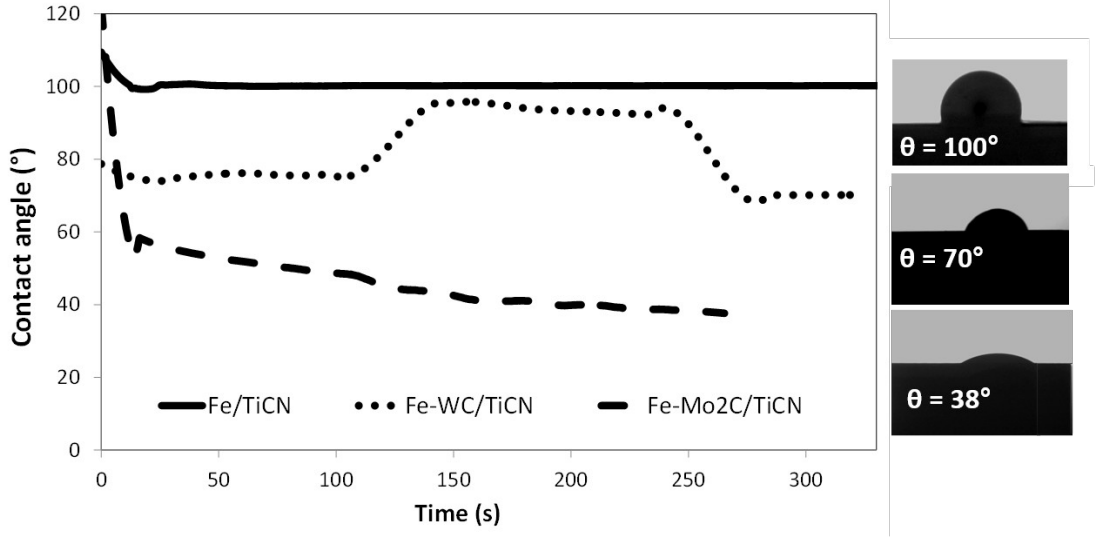

Figure 4. Evolution of contact angle regarding time of the metal/substrate systems: Fe/TiCN; Fe-6.2WC/TiCN and Fe-5.1Mo_2C/TiCN.

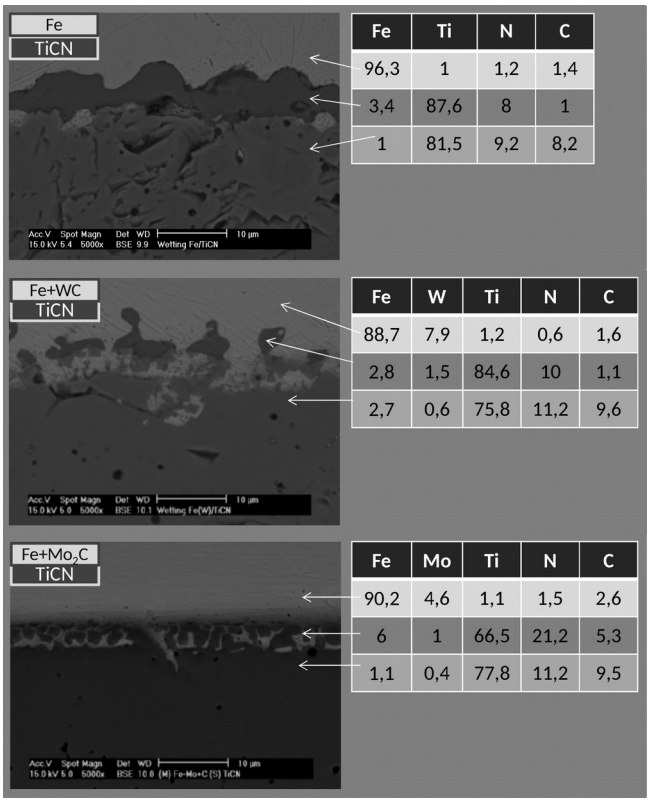

Fe	Ti	N	C
96,3	1	1,2	1,4
3,4	87,6	8	1
1	81,5	9,2	8,2

Fe	W	Ti	N	C
88,7	7,9	1,2	0,6	1,6
2,8	1,5	84,6	10	1,1
2,7	0,6	75,8	11,2	9,6

Fe	Mo	Ti	N	C
90,2	4,6	1,1	1,5	2,6
6	1	66,5	21,2	5,3
1,1	0,4	77,8	11,2	9,5

Figure 5. Interface of the systems (left side): Fe/TiCN; Fe-6.2WC/TiCN and Fe-4.8Mo_2C/TiCN after wetting experiments and EDX analysis of metallic sample, interface and TiCN substrate (right side). (All the compositions are expressed in wt. %).

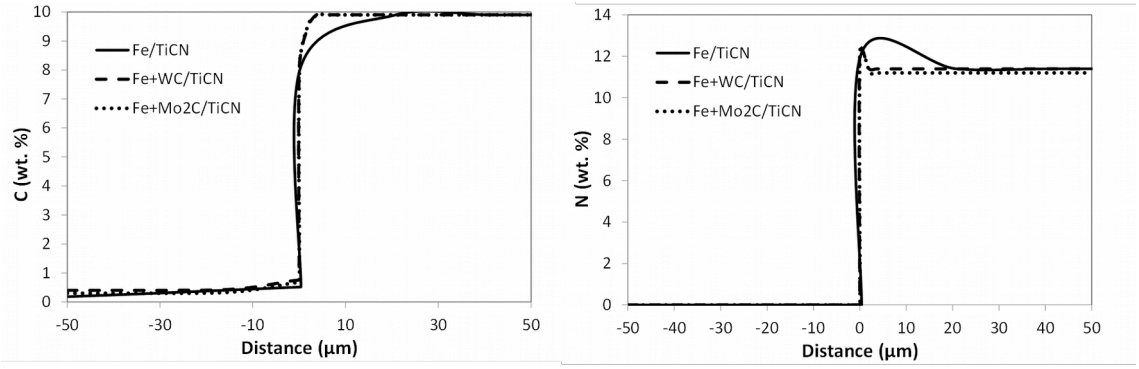

Figure 6. Evolution of the C and N wt. % at the interface for the systems Fe/TiCN; Fe-6.6WC/TiCN and Fe-5.1Mo_2C/TiCN simulated by Dictra software (at 1560 °C in a distance of 100 µm during 300 s).

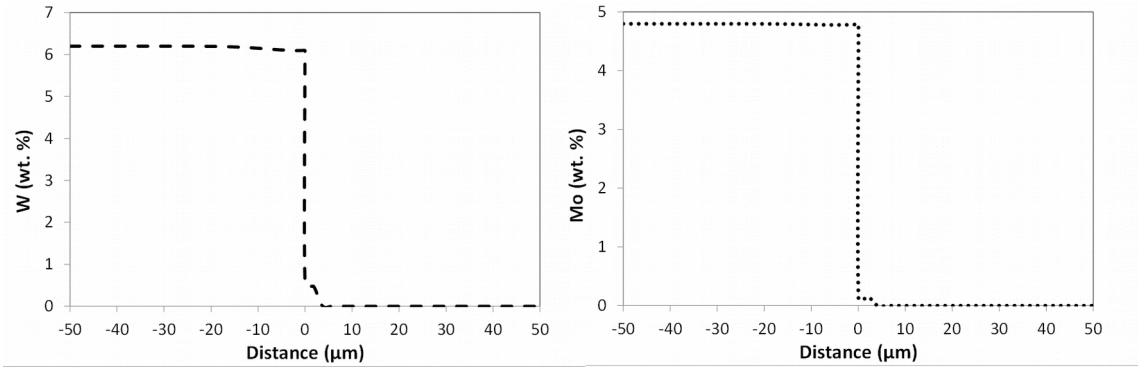

Figure 7. Evolution of the W and Mo wt. % at the interface of the systems Fe-6.6WC/TiCN and Fe-5.1Mo_2C/TiCN, respectively, simulated by Dictra software (at 1560 °C in a distance of 100 µm during 300 s).

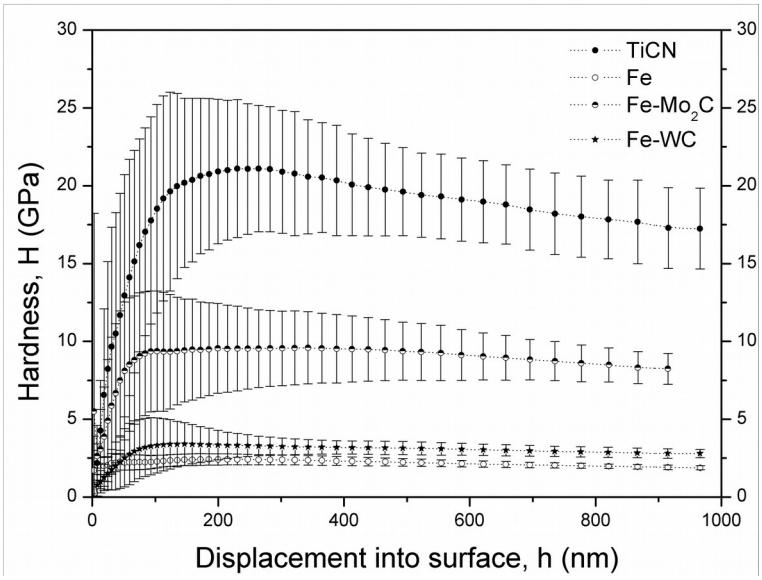

Figure 8. Hardness evolution for all the systems of study against the maximum displacement into surface.

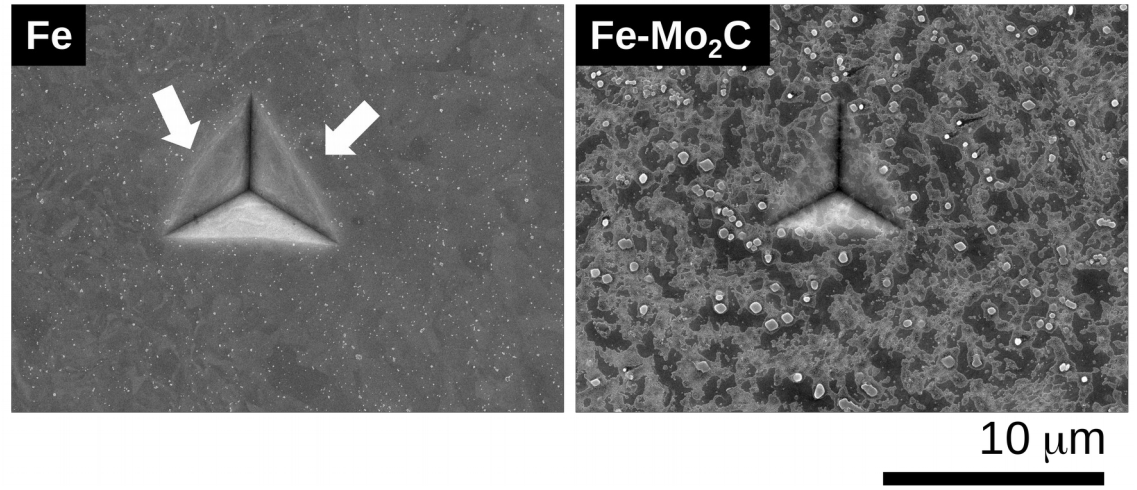

Figure 9. FESEM image of a residual imprint performed at 1000 nm of maximum displacement into surface for Fe and Fe-Mo_2C metallic systems.

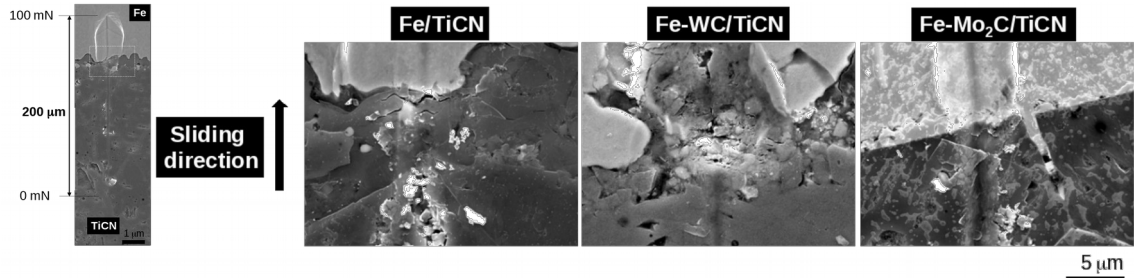

Figure 10. FESEM image for the nanoscratch track performed at incremental load from 0 to 100 mN (left hand side) for the Fe/TiCN system. Magnification of the main fracture events activated in the interface for all the systems investigated here done at constant load (100 mN).